Inorganic Chemistry

Article

pubs.acs.org/IC

Lattice-Modulated Phase Transition Coupled with Redox-Isomeric Interconversion of *o*-Semiquinone–Catecholato into Bis(*o*-semiquinonato) Cobalt Complexes

Michael P. Bubnov,*[†,‡] Nina A. Skorodumova,[†] Alla V. Arapova,[†] Natalia N. Smirnova,[‡] Maxim A. Samsonov,[†] Georgy K. Fukin,[†,‡] Vladimir K. Cherkasov,[†,‡] and Gleb A. Abakumov[†,‡]

[†]G. A. Razuvaev Institute of Organometallic Chemistry of RAS, 49 Tropinina str., GSP-445, 603950 Nizhny Novgorod, Russia

[‡]Lobachevsky State University of Nizhny Novgorod Gagarina av. 23/5, Nizhny Novgorod, 603950 Russia

Supporting Information

ABSTRACT: Two redox-isomeric (valence tautomeric) complexes (2,2′-bpy)-Co(3,6-DBSQ)$_2$ (**1**) and (1,10-phen)Co(3,6-DBSQ)$_2$ (**2**) (where 2,2′-bpy = 2,2′-dipyridine; 1,10-phen = 1,10-phenanthroline; 3,6-DBSQ = 3,6-di-*tert*-butyl-benzosemiquinone-1,2) reveal phase transitions that accompany redox-isomeric interconversions of semiquinone–catecholato isomer into a bis-(semiquinonato) one. Phase transitions differ one from another by thermodynamic parameters (transition temperature and interval, enthalpy, and entropy). Complexes **1** and **2** have the same crystal system and space group, and they form solid solutions with any molar ratio. The number of solid solutions with the molar ratios of 2:1, 1:1, 1:2, 1:4, 1:8, and 1:16 of **1** per **2**, respectively, were obtained. Product with 1:1 ratio was studied by precise calorimetry, by variable-temperature magnetic susceptibility, and by X-ray structural analysis. All solid solutions were investigated by means of differential scanning calorimetry. Each solid solution possesses phase transition whose parameters depend on its composition. Transition temperature and enthalpy gradually grow with increasing of molar fraction of **1**. The diagram "enthalpy–composition" is linear, whereas phase diagram "transition temperature–composition" is the bent-up arc.

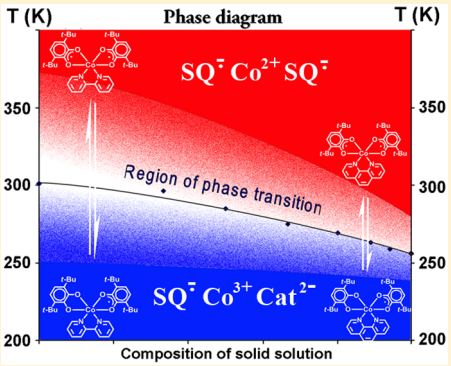

INTRODUCTION

In 1980 C. Pierpont reported that complex (2,2′-bpy)Co(3,5-DBSQ)$_2$ (where 2,2′-bpy = 2,2′-dipyridine and 3,5-DBSQ = 3,5-di-*tert*-butyl-benzosemiquinone-1,2) in solution exists as equilibrium mixture of isomers differing by valence and spin states of cobalt atom and quinonato ligand:[1]

$$\begin{gathered}(2,\,2'\text{-bpy})\mathrm{Co}^{3+}(3,\,5\text{-DBCat}^{2-})(3,\,5\text{-DBSQ}^{\cdot-}) \\ \mathrm{Co(III)},\ \mathrm{d}^6,\ \text{low spin} \\ \rightleftharpoons \\ (2,\,2'\text{-bpy})\mathrm{Co}^{2+}(3,\,5\text{-DBSQ}^{\cdot-})_2 \\ \mathrm{Co(II)},\ \mathrm{d}^7,\ \text{high spin}\end{gathered}$$

Later, a similar phenomenon occurring in solid phase was observed.[2,3] Since that time the redox-isomeric (valence tautomeric) transformations of semiquinonato cobalt complexes of general formula (N_N)Co("Q")$_2$ attracted attention of different scientific groups (N_N = nitrogen N-donor ligands, "Q" = mono (SQ) or dianions (Cat) of *o*-quinones).[4] It was shown that the conversion of redox isomers is followed by phase transition.[2] Phase transition was quantitatively characterized.[5] Its parameters depend on the redox potential of quinonato ligand[6] and on the nature of neutral ancillary ligand.[7] It should be mentioned that the influence of ancillary nitrogen donor is multiple varied. N-Donor ability coupled with π-electron acceptor property play the main role.[3,8] Structural flexibility of N-donor ligand modulates the entropy contribution into equilibrium constant.[9] Solvate molecules affect the lattice hardness and consequently in some cases dramatically influence on the redox-isomeric equilibrium.[3] In 2011 we published the detailed study of unsolvated (1,10-phen)Co(3,6-DBSQ)$_2$[7] (1,10-phen = 1,10-phenanthroline) and ascertained the difference between it and its benzene solvate.[8]

Here we reproduced the X-ray structural studies of complexes **1** and **2** at different temperatures and more thorough variable-temperature magnetic susceptibility studies of them. To understand the influence of lattice on the parameters of redox-isomeric transformation we obtained solid solution of **1** and **2** with 1:1 molar ratio (**3**). Solid phase **3** was studied by X-ray diffraction study also by variable-temperature magnetic susceptibility and precise adiabatic vacuum calorimetry measurements. We investigated the phase transitions occurring in the number of solid solutions of **1** and **2** of different compositions by differential scanning calorimetry (DSC) technique.

It should be mentioned that preparation and studies of solid solutions of compounds undergoing entropy-driven intercon-

Received: April 3, 2015
Published: July 31, 2015

DOI: 10.1021/acs.inorgchem.5b00716
Inorg. Chem. 2015, 54, 7767–7773

Table 1. Crystallographic Data and Structure Refinement Details for 1a−3b

	1a	1b	2a	2b	3a	3b
formula	$C_{38}H_{48}CoN_2O_4$		$C_{40}H_{48}CoN_2O_4$		$C_{39}H_{47}CoN_2O_4$	
FW	655.71		679.73		666.72	
space group, Z	$C2/c$, 4	$C2/c$, 4	$C2/c$, 4	$C2/c$, 4	$C2/c$, 4	$C2/c$, 4
T, K	100(2)	340(2)	240.0(2)	281.0(2)	100(2)	375(2)
a, b, c, Å	10.6666(4)	10.8586(4)	10.6356(6)	10.6017(5)	10.64542(12)	10.7557(5)
	29.4989(10)	30.4249(9)	30.7654(14)	31.7284(15)	29.8999(3)	31.4355(10)
	11.9245(4)	12.2200(5)	12.2285(8)	12.2126(7)	12.07078(16)	12.3761(7)
β, deg	112.564(4)	114.525(5)	113.438(7)	114.634(6)	112.5063(15)	115.365(7)
V, Å^3	3464.9(2)	3672.9(2)	3671.1(4)	3734.1(3)	3549.47(7)	3781.1(3)
d_c, g/cm^3	1.257	1.186	1.230	1.209	1.250	1.173
μ(Mo Kα), mm^{-1}	0.536	0.506	0.509	0.500	0.525	0.493
θ-range, deg	2.93 to 30.00	2.88 to 30.00	2.93 to 30.00	3.16 to 30.00	2.91 to 30.00	3.17 to 30.00
I_{hkl} coll/uniq R_{int}	19 700/5042	36 797/5349	36 772/5328	35 737/5437	164 653/5129	38 693/5495
	0.0648	0.0881	0.0760	0.0762	0.0378	0.0514
data/N	5042/210	5349/210	5328/219	5437/219	5129/219	5495/219
GOF	1.017	0.994	0.988	0.950	1.037	1.049
R_1 for $I > 2\sigma_I$ wR_2	0.0494	0.0649	0.0544	0.0549	0.0302	0.0721
	0.0844	0.1474	0.1242	0.1152	0.0815	0.1892
R_1 for all data wR_2	0.0822	0.1480	0.0935	0.1135	0.0330	0.1463
	0.0920	0.1769	0.1392	0.1361	0.0836	0.2214

versions such as redox-isomerism (valence tautomerism)[10] and spin-crossover[11] was already described in literature. The attention of the authors was focused on the effects of dilution of converting molecules by isomorphic inert molecules. The main distinction of our approach from previously described ones is the using of both interconverting components and preparing of the solid solutions of redox-isomeric compound in the other redox-isomeric one.

EXPERIMENTAL SECTION

General Remarks. All the synthetic procedures were performed in evacuated ampules using specially prepared solvents without oxygen and moisture. All the initial substances are commercially available. Magnetochemical measurements were performed on a Quantum Design MPMS-5S SQUID magnetometer in the temperature range of 2−350 K at a magnetic field of 5000 Oe.

Synthesis. Complex Co(3,6-DBSQ)$_3$ was prepared as described in ref 12. Warm solution of Co(3,6-DBSQ)$_3$ in diethyl ether (1.0 mmol) was quickly mixed with warm solution of the mixture 2,2′-bpy (x mmol) and 1,10-phen (1 − x mmol) in diethyl ether (x = 0.67; 0.5; 0.33; 0.2; 0.11; 0.06). Ampoule was kept immovable and allowed to be cooled slowly (∼1−2 h) to room temperature. The color of the solution changed from dark blue-green to dark olive. The dark well-faceted crystals were separated by filtration and dried in vacuum. Yield: 0.407−0.479 g (62−73)%.

X-ray Crystallography. The X-ray data for **1a**−**1c**, **2a**, **2b**, **3a**, **3b** were collected on Agilent Xcalibur EOS diffractometer. The structures were solved by direct methods and were refined on F2 using SHELXTL package.[13] All the hydrogen atoms were placed in calculated positions and were refined in the riding model. ABSPACK (CrysAlis Pro)[14] was used to perform area-detector scaling and absorption corrections. The details of crystallographic, collection, and refinement data are shown in Table 1, and corresponding cif files are available as Supporting Information.

Precise Adiabatic Vacuum Calorimetry and Differential Scanning Calorimetry. A fully automated BKT-3 adiabatic vacuum calorimeter, designed and produced by CJSC Termis (Mendeleevo, Moscow region), was used to study the temperature dependence of heat capacity of sample of solid phase **3**, which is solid solution product (1:1), in the range of 85−350 K. The design of the calorimeter and the operating procedure were analogous to those described previously.[15,16] It was established that the apparatus and method of measurement allowed us to obtain the heat capacity values of condensed substances with an accuracy of ±0.2% in the range from 40 to 350 K; and to measure the temperatures of physical transformations with an accuracy of ±0.01 K, in accordance with ITS-90. Enthalpy of transformation for **2** was precisely evaluated by the continuous energy supply technique; its entropy was calculated as $\Delta_{tr}H^\circ/T$ because of the closeness of its shape to the first-order transition.[7] Transition enthalpy and entropy for **1** and **3** were calculated graphically from the area between anomalous and normal trends of the curves $C^\circ_{p,m} = f(T)$ and $C^\circ_{p,m} = f(\ln T)$, respectively, as customary for transitions of this type.[5]

A differential scanning calorimeter DSC 204 F1 Phoenix (Netzsch, Geraetebau, Germany) was used to investigate **1**, **2**, and solid solutions in the range of 200−380 K. The design of the DSC 204 F1 calorimeter and the measurement procedure were described, for example, in refs 15 and 16. The reliability of the calorimeter was checked by standard calibration experiments[17] to measure the thermodynamic characteristics for the melting of cyclohexane, mercury, indium, tin, lead, bismuth, and zinc. Temperature and enthalpy of transitions were estimated according to Netzsch Software Proteus.[18] The shape of DSC curves inside the temperature interval of transition depends on the composition of samples. Increasing the fraction of complex **1** in the composition leads to more gradual shape of DSC curve. So, the uncertainty of determination of the temperature and enthalpy of transitions increases with growing of fraction of **1**. The inaccuracy of temperature definition changes from ±1 K for pure **2** to ±5 K for pure **1**; the inaccuracy of enthalpy definition changes from 3% for pure **2** to 7% for pure **1**. The entropy of transition was not evaluated because of evident uncertainty of its determination. Measurements of thermophysical characteristics were conducted at an average rate of heating of a crucible containing the substance at 5 K/min in an argon flow of 20 mL/min. Most of the parameters were kept identical during all measurements: argon flow, initial temperature, heating rate, weight of the crucible and its cover, and the position of the crucible on the sensor.

RESULTS AND DISCUSSION

Complexes (2,2′-bpy)Co(3,6-DBSQ)$_2$ (complex **1**) and (1,10-phen)Co(3,6-DBSQ)$_2$ (complex **2**) were obtained by the reaction of tris(semiquinonato) precursor with neutral N-donor ligand as described earlier.[2,7]

DOI: 10.1021/acs.inorgchem.5b00716
Inorg. Chem. 2015, 54, 7767−7773

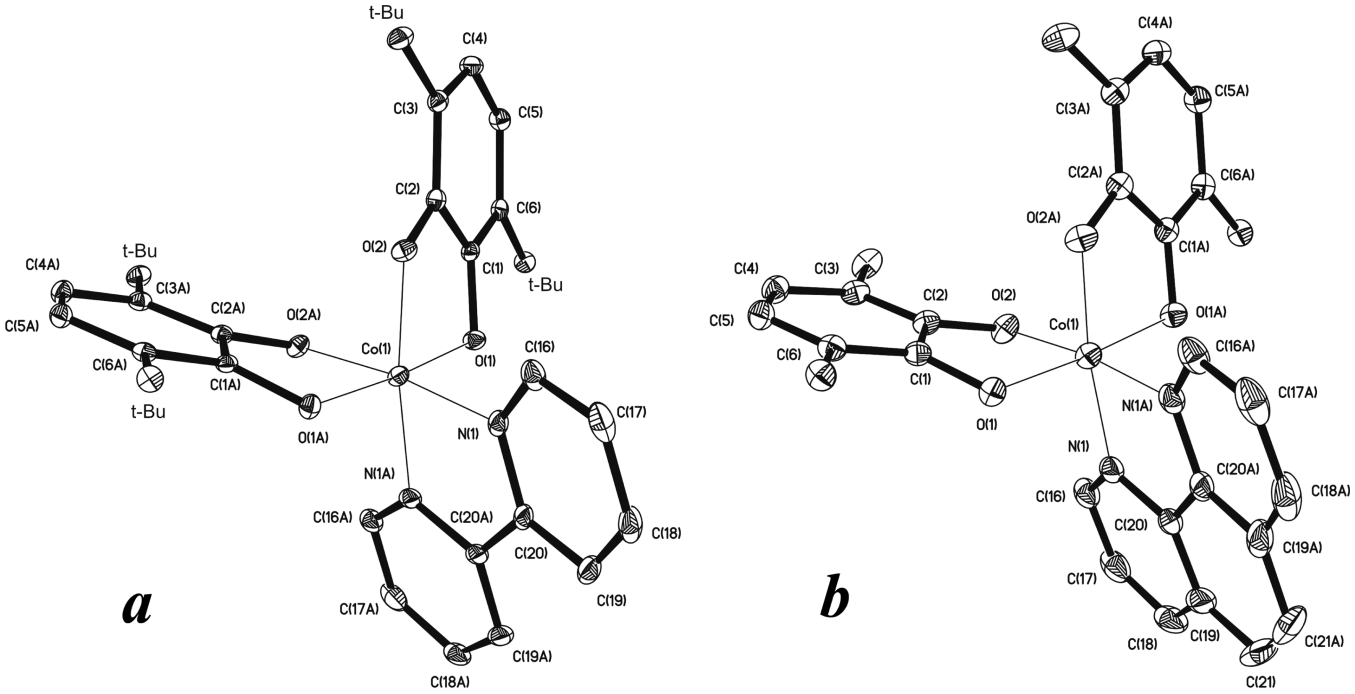

Figure 1. Common view of complexes **1a**, **1b** (a) and **2a**−**3b** (b). The occupation of C(21) atom is 0.5 in complex **3a**, **3b**. Symmetry transformations used to generate equivalent atoms: $-x, y, -z + 1/2$ in **1a**−**3b**.

Scheme 1. Synthesis of Complexes 1 and 2

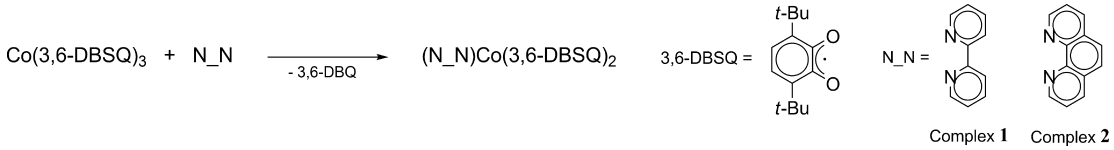

Scheme 2. Synthetic Procedure for Obtaining of the Solid Solutions

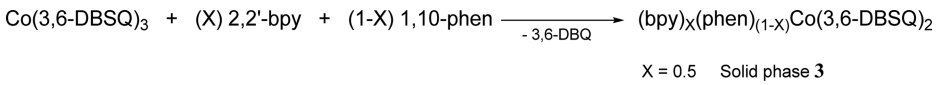

Scheme 3. Structural Formulas and Unit Cell Parameters of Complexes 1b (340 K) and 2b (281 K)

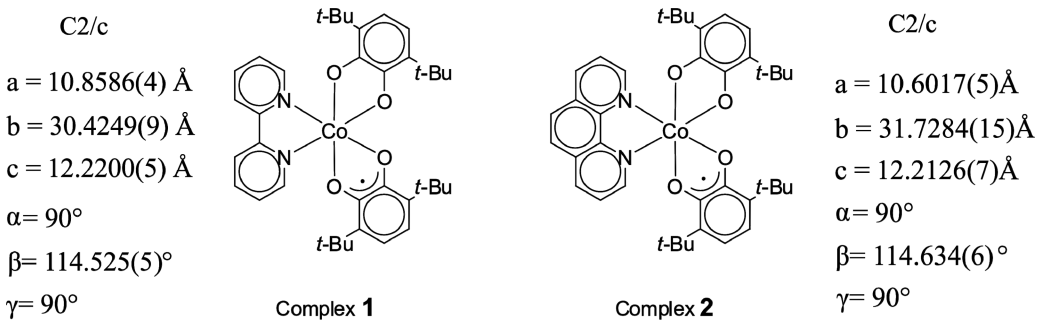

Using the mixture of neutral ligands with known molar ratio in the synthetic procedure (Scheme 2) performed in diethyl ether leads to crystalline products, which are solid solutions of complexes **1** and **2** reproducing the initial molar ratio of ligands. The product containing **1** and **2** in equal molar amounts (which was studied in detail) was denominated as **3** for brevity.

The product of cocrystallization **3** (with molar ratio of **1**:**2** as 1:1) was characterized by single-crystal X-ray crystallography. The structures of complexes **1** and **2** have been published previously.[2,7] Here we reproduced these experiments, and we would like to focus our attention on comparative analysis of the geometric parameters of crystalline phase **3** with **1** and **2**. It is known that complexes **1** and **2** undergo phase transition, which accompanies redox isomeric interconversion. Structural characteristics of both complexes **1**, **2**, and solid phase **3** change upon the transition. So, it is more correct to compare structural features below and above the transition range in temperature scale. X-ray study was performed at two temperatures: lower

DOI: 10.1021/acs.inorgchem.5b00716
Inorg. Chem. 2015, 54, 7767−7773

Table 2. Selected Bonds Lengths and Angles in Complexes 1a−3b

	complexes					
	low-temperature phase			high-temperature phase		
bond and angle	**1a**, 100 K	**3a**, 100 K	**2a**, 240 K	**1b**, 340 K	**3b**, 375 K	**2b**, 281 K
Co(1)−O(1)	1.8747(9)	1.8750(6)	1.880(1)	1.999(2)	2.021(2)	1.986(1)
Co(1)−O(2)	1.8636(9)	1.8639(5)	1.869(1)	2.002(2)	2.040(2)	2.009(1)
Co(1)−N(1)	1.940(1)	1.9443(6)	1.957(1)	2.057(2)	2.103(2)	2.075(1)
O(1)−C(1)	1.329(2)	1.3256(8)	1.322(2)	1.291(2)	1.282(2)	1.296(2)
O(2)−C(2)	1.332(2)	1.3296(9)	1.337(2)	1.283(3)	1.273(3)	1.293(2)
C(1)−C(2)	1.432(2)	1.4331(9)	1.434(2)	1.451(3)	1.477(3)	1.457(2)
C(2)−C(3)	1.416(2)	1.419(1)	1.412(2)	1.443(3)	1.428(3)	1.437(2)
C(3)−C(4)	1.386(2)	1.390(1)	1.384(2)	1.354(3)	1.342(4)	1.361(2)
C(4)−C(5)	1.403(2)	1.408(1)	1.403(2)	1.405(3)	1.415(4)	1.412(2)
C(5)−C(6)	1.385(2)	1.391(1)	1.380(2)	1.369(3)	1.359(3)	1.366(2)
C(6)−C(1)	1.415(2)	1.418(1)	1.416(2)	1.427(3)	1.422(3)	1.427(2)
O(1)Co(1)O(2)	87.14(4)	87.17(2)	86.85(4)	80.01(6)	78.94(6)	80.79(4)

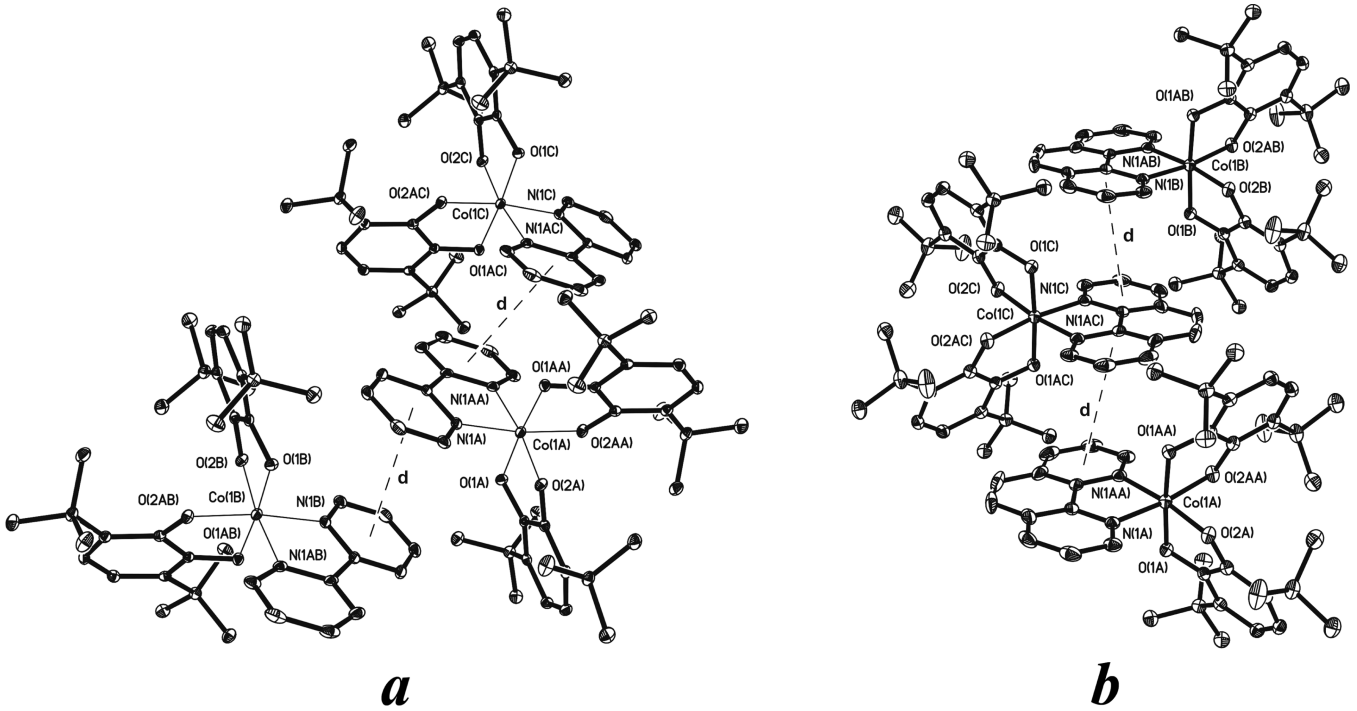

Figure 2. Distances between parallel centroids based on pyridine rings of adjacent complex molecules of **1** (a), **2**, and **3** (b).

Table 3. Selected Geometric Parameters of Complexes 1a−3b

	complexes					
	low-temperature phase			high-temperature phase		
geometric parameters	**1a**, 100 K	**3a**, 100 K	**2a**, 240 K	**1b**, 340 K	**3b**, 375 K	**2b**, 281 K
angle N(1)Co(1)N(1A)	82.45(7)	82.98(4)	83.72(7)	77.4(1)	78.4(1)	79.08(8)
torsion angle N(1)C(20)C(20A)N(1A)	9.4	7.2	5.5	7.6	6.6	4.9
distance between centroids (pyridine rings)	3.617 Å	3.635 Å	3.604 Å	3.731 Å	3.673 Å	3.571 Å

and higher than temperature range of coexisting of redox isomers. They are for complex **1** 100 K − **1a**, 340 K − **1b** (Figure 1a), for complex **2** 240 K − **2a**, 281 K − **2b** (Figure 1b), and for solid phase **3** (which is solid solution of complexes **1** and **2** with molar ratio 1:1) 100 K − **3a** and 375 K − **3b** (Figure 1b). (The reason why the temperature interval for structural measurements of complex **2** was chosen so small compared to **1** and **3** will be the subject of special report.)

As with complexes **1** and **2** (Figure 1a,b) the Co atom in **3** has a distorted octahedral coordination core and lies on the C_2 axis (Figure 1b). As a consequence the geometric parameters of Cat and SQ ligands in low-temperature phase (in **3a**) are identical. The Co(1)−O(1,2) and Co(1)−N(1) distances in **3a** are slightly shorter as compared to analogous distances in **3b** (Table 2), which is a consequence of change of cobalt atom spin state and charge distribution between cobalt atom and

DOI: 10.1021/acs.inorgchem.5b00716
Inorg. Chem. 2015, 54, 7767−7773

quinonato ligand (redox-isomeric interconversion).[19] The same trends take place in complexes **1a−b** and **2a−b** (Table 2).

The peculiarity of molecular structures is slight twist of pyridine fragments one relative to another in both dipyridine and phenanthroline ligands in **1a,b**, **2a,b**, and **3a,b**. Each pyridine fragment is parallel to its counterpart pyridine fragment of the adjacent molecule in the stairway (Figure 2). The torsion angles N(1)C(20)C(20A)N(1A), which characterize the twist of pyridine fragments one relative to another one and the distances between centroids based on each pyridine of adjacent molecules (Figure 2) are listed in Table 3. Interesting to note that the values of the angles N(1)Co(1)N(1A) and N(1)C(20)C(20A)N(1A) in **3a** and **3b** have the average values between the same angles in **1a** and **2a** (**1b** and **2b**), respectively, for both low- and high-temperature phases (Table 3). The same feature can be observed for distance between centroids calculated for pyridine rings of parallel ancillary ligands of adjacent molecules in staircase (Table 3, Figure 2).

The X-ray crystallography confirms the forming of solid solution of complexes **1** and **2**. Complexes **1** and **2** differ one from another only by ancillary ligand: 2,2′-bpy in **1** and 1,10-phen in **2**. These ancillary ligands differ one from another by two carbon atoms: C(21) and C(21A). The occupation of C(21) and C(21A) in crystalline phases **3a**, **3b** is 0.5. It means that molar fractions of complexes **1** and **2** in solid phase **3** are approximately equal. The analysis of molecular and crystalline structural parameters at different temperatures (**3a**, **3b**) provides evidence about temperature-driven redox-isomeric interconversion occurring in solid solution **3**.

The most widespread method of characterization of redox-isomeric transition is the temperature-variable magnetic susceptibility measurement. The $\chi T - T$ dependence directly reflects the molar fraction of high-temperature redox-isomer. Magnetic moment temperature dependences for both complexes **1** and **2** were already reported.[2,7] We thoroughly reproduced these experiments and measured temperature dependences of magnetic susceptibility of crystalline phase **3** and mechanical mixture of complexes **1** and **2** in 1:1 molar ratio. The results are presented in Figure 3. All the dependences demonstrate small temperature hysteresis (~4 K). The same value of hysteresis was observed earlier in similar complex (phen)Co(3,5-DBSQ)$_2$·toluene.[3] One can see that the curve $\mu_{eff} - T$ for mechanical mixture seems to be the average of temperature dependences for complexes **1** and **2**. It differs from $\mu_{eff} - T$ dependence obtained for crystalline phase **3**, which is the solid solution of complexes **1** and **2** in the same 1:1 molar ratio. Note that the magnetic curve for **3** is essentially closer to that for complex **1** than for **2**. This observation will be discussed below.

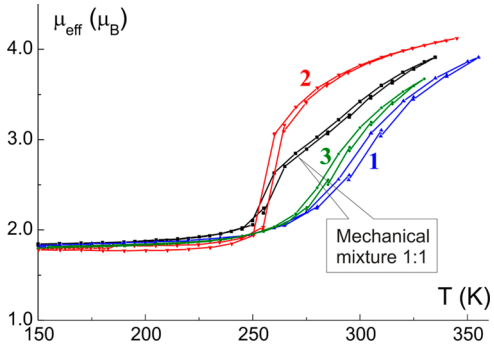

Figure 3. Fragments of temperature dependences of magnetic moments of complexes **1**, **2**, solid phase **3**, and mechanical mixture of **1** and **2** in 1:1 molar ratio.

Phase transitions accompanying redox-isomeric interconversions in complexes **1** and **2** were previously studied by precise adiabatic vacuum calorimetry.[5,7] Parameters of phase transitions are listed here:

Complex **1**:

$$(2,\ 2'\text{-bpy})Co^{3+}(3,\ 6\text{-DBCat}^{2-})(3,\ 6\text{-DBSQ}^{-}) \rightleftharpoons (2,\ 2'\text{-bpy})Co^{2+}(3,\ 6\text{-DBSQ}^{-})_2$$

T_{tr} = 299.6 ± 0.5 K, interval 250−375 K, $\Delta H°$ =15.0 ± 0.1 kJ/mol; $\Delta S°$ = 48.05 ± 0.4 J/mol·K.

Complex **2**:

$$(1,\ 10\text{-phen})Co^{3+}(3,\ 6\text{-DBCat}^{2-})(3,\ 6\text{-DBSQ}^{-}) \rightleftharpoons (1,\ 10\text{-phen})Co^{2+}(3,\ 6\text{-DBSQ}^{-})_2$$

T_{tr} = 254.5 ± 0.1, interval 240−281 K, $\Delta H°$ = 6.320 ± 0.08 kJ/mol; $\Delta S°$ = 24.8 ± 0.3 J/mol·K.

Transition occurring in complex **1** is smooth and has larger enthalpy when compared to that in **2**. Analogous transition in complex **2** is abrupt and has lower enthalpy. Decreasing transition temperature and enthalpy when coming from complex **1** to **2** is coupled with enlarging of aromatic system of ancillary ligand at the same complex composition and structure. It is caused by more strong π-acceptor properties of 1,10-phen compared to 2,2′-dipyridyl. The reduction potential of 2,2′-bpy ($E_{1/2}$ = −2.13 V) is more negative in comparison with 1,10-phen ($E_{1/2}$ = −1.99 V).[20] At the same time the N-donor abilities (which can be evaluated with the help of acidity) of both ligands are close: pK_a(2,2′-bpy) = 4.23; pK_a(1,10-phen) = 4.27.[21] A different slope of transitions (sharp for **1** and smooth for **2**) seems to be caused by different $\pi-\pi$ interligand coupling. The peculiarity of crystal structure of both complexes is stacking of neutral ligands of adjacent molecules to form a stairway (Figure 2). Pyridine fragments of the adjacent molecules are parallel and situated one above the other with shift (Figure 2). Taking into account the extended π-system of phenanthroline compared to dipyridine, the overlap of their planes in the stack is larger in the case of phenanthroline. The distances between corresponding centroids (see Table 3) are shorter in **2**. So, the interaction along the chain in **2** should be stronger. As a consequence the transition in **2** occurs more cooperatively.[22]

Crystalline phase **3** was also investigated by precise adiabatic vacuum calorimetry. Figure 4 presents the temperature dependence of heat capacity of crystalline phase **3** compared to that for **1** and **2**.

Thermodynamic parameters of phase transition in crystalline phase **3** determined by precise calorimetry are the average between corresponding magnitudes reported for pure complexes with the exception of temperature (Table 4). Transition temperature of solid solution **3** determined as maximal deviation of heat capacity by precise adiabatic vacuum calorimetry is 285.8 K, whereas the average value between T_{tr} of **1** and **2** is 276.7 K. So, the transition temperature of **3** is closer to that of complex **1** as was already shown by magnetic measurements.

The solid solutions with the other ratios of complexes **1** and **2** were investigated by DSC. General view of DSC curves is

DOI: 10.1021/acs.inorgchem.5b00716
Inorg. Chem. 2015, 54, 7767−7773

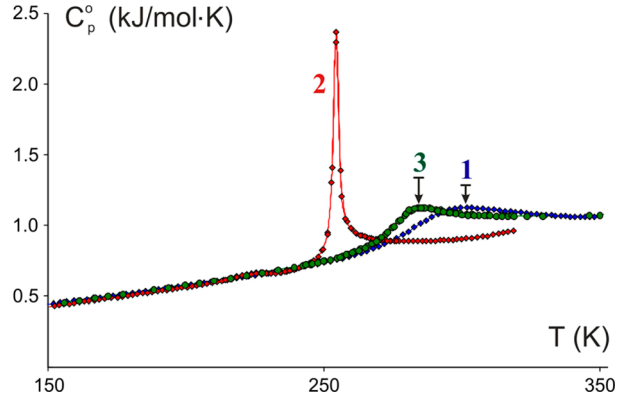

Figure 4. Temperature dependences of heat capacity of complexes **1**, **2** (cited from refs 5 and 7), and crystalline phase **3**, which is solid solution of **1** and **2** with 1:1 molar ratio.

Table 4. Thermodynamic Parameters of Phase Transitions Occurring in Complexes 1, 2, and Solid Solution 3 in Comparison with Averaged Values

value/solid	complex **1**	solid solution **3**	average between **1** and **2**	complex **2**
T_{tr} (K)	299.6 ± 0.5	285.8 ± 0.5	276.7	254.5 ± 0.1
$\Delta H°$ (kJ/mol)	14.96 ± 0.1	10.69 ± 0.1	10.64	6.32 ± 0.1
$\Delta S°$ (J/mol K)	48.05 ± 0.4	36.8 ± 0.3	36.8	24.8 ± 0.3

presented in the Figure 5. Experimental data determined by DSC for complexes **1**, **2**, and 1:1 (**1**:**2**) solid solution (i.e., **3**)

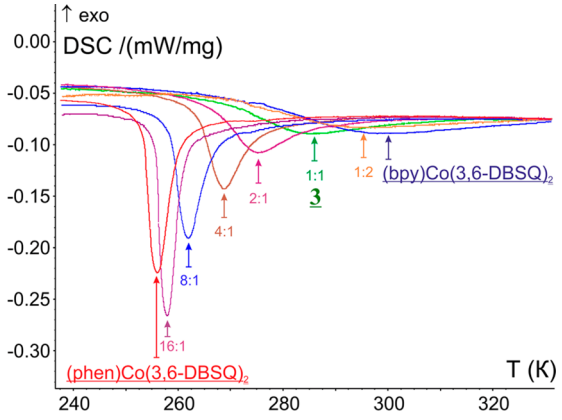

Figure 5. DSC curves of solid solutions of complexes **1** and **2** with different ratios.

are in agreement with results obtained by precise adiabatic vacuum calorimetry. Note that transition temperature and sharpness permanently change with increasing of the molar fraction of **1** in the lattice of **2**. So, the transition temperature and enthalpy gradually grow with enlarging of molar fraction of complex **1** (Table 5). Using the DSC data, the diagrams "*transition temperature*–*composition*" and "*transition enthalpy*–*composition*" were drawn (Figures 6 and 7, respectively).

The diagram "*transition temperature*–*composition*" is phase diagram. The curve (exactly the region) subdivides the field of complex existing into two parts: the area of semiquinone–catecholato form and the area of bis(semiquinonato) form of complexes. Below the curve (region) the catecholate–semiquinonato redox-isomer exists, whereas above the curve (region) the bis(semiquinonato) redox-isomer exists. The area inside the region close to the curve corresponds to equilibrium between them.

Table 5. Thermodynamic Parameters of Phase Transition Accompanying Redox-Isomeric Interconversion of Catecholate–Semiquinonato Form into Bis(semiquinonato) Form of Complexes 1 and 2 in the Number of Solid Solutions of Complexes 1 and 2 with Different Ratios

sample	T_{tr} (K)	$\Delta_{tr}H°$ (kJ/mol)
(bpy)Co(3,6-DBSQ)$_2$ (**1**)	301 ± 5	14.5 ± 1.00
solid solution 1:2 (of **2**:**1**)	296 ± 4	12.2 ± 0.80
solid solution 1:1	285 ± 3	10.2 ± 0.60
solid solution 2:1	275 ± 2	9.20 ± 0.46
solid solution 4:1	269 ± 1	7.74 ± 0.31
solid solution 8:1	263 ± 1	7.31 ± 0.22
solid solution 16:1	259 ± 1	6.54 ± 0.20
(phen)Co(3,6-DBSQ)$_2$ (**2**)	256 ± 1	6.31 ± 0.19

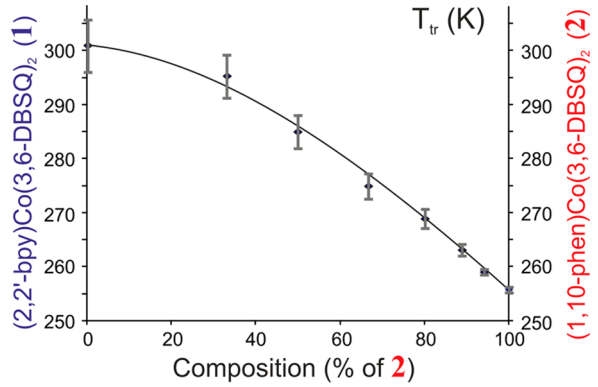

Figure 6. Diagram "*transition temperature*–*composition*" for the number of solid solutions of complexes **1** and **2** (measurement uncertainty is displayed for each point).

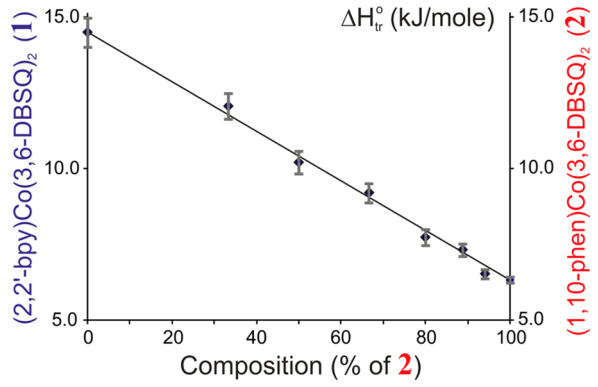

Figure 7. Diagram "*transition enthalpy*–*composition*" for the number of solid solutions of complexes **1** and **2** (solid line reflects the best fit approximation line; measurement uncertainty is displayed for each point.).

It becomes clear why the transition temperature of the solid solution 1:1, namely, solid phase **3** is closer to T_{tr} of **1** than of T_{tr} of **2**. The diagram "*transition temperature*–*composition*" is the bent-up arc in contrast to diagram "*transition enthalpy*–*composition*", which is linear with correlation coefficient R^2 = 0.9945.

DOI: 10.1021/acs.inorgchem.5b00716
Inorg. Chem. 2015, 54, 7767–7773

CONCLUSION

Isostructural complexes (2,2′-bpy)Co(3,6-DBSQ)$_2$ and (1,10-phen)Co(3,6-DBSQ)$_2$ possessing redox-isomeric properties form solid solutions with any ratio. Structural parameters (intra- and intermolecular distances and angles) measured in solid solution containing mentioned complexes in equimolar amounts have average values between that determined in pure complexes. Magnetic susceptibility and heat capacity temperature dependences indicate that the redox-isomeric transition temperature for solid solution 1:1 is closer to that for complex (2,2′-bpy)Co(3,6-DBSQ)$_2$. Investigation of solid solutions of the number of different compositions by DSC techniques indicates that the sharpness and the temperature of transition correlate with solid solution composition. Diagram "*enthalpy−composition*" is linear, whereas phase diagram "*transition temperature−composition*" is bent-up arc. The last observation allows the conclusion that coupling of two different complexes in one lattice stabilizes the low-temperature semiquinonate−catecholato redox-isomer because the square of it existence in coordinates "*transition temperature−composition*" enlarges. Co-crystallization of isomorphic complexes can serve for fine-tuning of redox-isomeric transition parameters.

ASSOCIATED CONTENT

Supporting Information

Illustrations of crystallographic structures with corresponding parameters, crystallographic data and structures in CIF files, and crystallographic data in text files. The Supporting Information is available free of charge on the ACS Publications website at DOI: 10.1021/acs.inorgchem.5b00716. CCDC **1a** − 1056346, **1b** − 1056347, **2a** − 1056348, **2b** − 1056349, **3a** − 1056350, **3b** − 1056351 contain the supplementary crystallographic data for this paper. These data can be obtained free of charge from The Cambridge Crystallographic Data Centre via ccdc.cam.ac.uk/products/csd/request/request.php4.

AUTHOR INFORMATION

Corresponding Author

*Phone: +7 831 4627682. Fax: +7 831 4627497. E-mail: bmp@iomc.ras.ru.

Notes

The authors declare no competing financial interest.

ACKNOWLEDGMENTS

The authors are grateful to A. Bogomyakov (International Tomography Center, Novosibirsk) for magnetic measurements. This work was financially supported by the Russian Foundation for Basic Research (Project No. 13-03-12444-ofi-m2), the Council on Grants at the President of the Russian Federation (Program for State Support of Leading Scientific Schools of the Russian Federation, Grant NSh-271.2014.3). The work was partly supported by the grant (the agreement of August 27, 2013 No. 02.B.49.21.0003 between The Ministry of education and science of the Russian Federation and Lobachevsky State Univ. of Nizhni Novgorod).

REFERENCES

(1) Buchanan, R. M.; Pierpont, C. G. *J. Am. Chem. Soc.* **1980**, *102*, 4951−4957.

(2) Abakumov, G. A.; Cherkasov, V. K.; Bubnov, M. P.; Ellert, O. G.; Dobrokhotova, Z. V.; Zakharov, L. N.; Struchkov, Y. T. *Dokl. Akad. Nauk SSSR* **1993**, *330*, U669.

(3) (a) Adams, D. M.; Dei, A.; Rheingold, A. L.; Hendrickson, D. N. *Angew. Chem., Int. Ed. Engl.* **1993**, *32*, 880. (b) Adams, D. M.; Dei, A.; Rheingold, A. L.; Hendrickson, D. N. J. *J. Am. Chem. Soc.* **1993**, *115*, 8221−8229.

(4) (a) Evangelio, E.; Ruiz-Molina, D. *C. R. Chim.* **2008**, *11*, 1137−1154. (b) Sato, O.; Tao, J.; Zhang, Y.-Z. *Angew. Chem., Int. Ed.* **2007**, *46*, 2152−2187. (c) Hendrickson, D. N.; Pierpont, C. G. *Top. Curr. Chem.* **2004**, *234*, 63−95.

(5) Lebedev, B. V.; Smirnova, N. N.; Abakumov, G. A.; Cherkasov, V. K.; Bubnov, M. P. *J. Chem. Thermodyn.* **2002**, *34*, 2093−2103.

(6) (a) Arapova, A. V.; Bubnov, M. P.; Abakumov, G. A.; Cherkasov, V. K.; Skorodumova, N. A.; Smirnova, N. N. *Russ. J. Phys. Chem. A* **2009**, *83*, 1257−1261. (b) Abakumov, G. A.; Bubnov, M. P.; Cherkasov, V. K.; Skorodumova, N. A.; Arapova, A. V.; Smirnova, N. N. *Russ. J. Phys. Chem. A* **2008**, *82*, 172−176.

(7) Bubnov, M. P.; Skorodumova, N. A.; Bogomyakov, A. S.; Romanenko, G. V.; Arapova, A. V.; Kozhanov, K. A.; Smirnova, N. N.; Abakumov, G. A.; Cherkasov, V. K. *Russ. Chem. Bull.* **2011**, *60*, 449−455.

(8) Jung, O.-S.; Pierpont, C. G. *J. Am. Chem. Soc.* **1994**, *116*, 1127−1128.

(9) Jung, O.-S.; Jo, D. H.; Lee, Y.-A.; Sohn, Y. S.; Pierpont, C. G. *Inorg. Chem.* **1998**, *37*, 5875−5880.

(10) Dei, A.; Poneti, G.; Sorace, L. *Inorg. Chem.* **2010**, *49*, 3271−3277.

(11) (a) Tayagaki, T.; Galet, A.; Molnar, G.; Munoz, M. C.; Zwick, A.; Tanaka, K.; Real, J.−A.; Bousseksou, A. *J. Phys. Chem. B* **2005**, *109*, 14859−14867. (b) Martin, J.−P.; Zarembowitch, J.; Bousseksou, A.; Dworkin, A.; Haasnoot, J. G.; Varret, F. *Inorg. Chem.* **1994**, *33*, 6325−6333. (c) Baldé, C.; Desplanches, C.; Gütlich, P.; Freysz, E.; Létard, J. F. *Inorg. Chim. Acta* **2008**, *361*, 3529−3533. (d) Balde, C.; Desplanches, C.; Wattiaux, A.; Guionneau, P.; Gutlich, P.; Letard, J.-F. *Dalton Trans.* **2008**, 2702−2707.

(12) Lange, C. W.; Conklin, B. J.; Pierpont, C. G. *Inorg. Chem.* **1994**, *33*, 1276.

(13) Sheldrick, G. M. *SHELXTL* v.6.12, Structure Determination Software Suite; Bruker AXS: Madison, WI, 2000.

(14) Agilent Technologies. *CrysAlis Pro;* Agilent Technologies Ltd: Yarnton, England, 2011.

(15) Varushchenko, R. M.; Druzhinina, A. I.; Sorkin, E. L. *J. Chem. Thermodyn.* **1997**, *29*, 623.

(16) Malyshev, V. M.; Mil'ner, G. A.; Sorkin, E. L.; Shibakin, V. F. *Prib. Tekh. Eksp.* **1985**, *6*, 195.

(17) Honhe, G. W. H.; Hemminger, W. F.; Flammersheim, H. F. *Differential Scanning Calorimetry;* Spriger-Verlag: Berlin, Germany, 2003.

(18) Drebushak, V. A. *J. Therm. Anal. Calorim.* **2004**, *76*, 941.

(19) Jung, O.-S.; Pierpont, C. G. *Inorg. Chem.* **1994**, *33*, 2227−2235.

(20) Krishnan, C. V.; Creutz, C.; Schwarz, H. A.; Sutin, N. *J. Am. Chem. Soc.* **1983**, *105*, 5617−5623.

(21) Albert, A.; Goldacre, R.; Phillips, J. *J. Chem. Soc.* **1948**, 2240.

(22) Sorai, M.; Seki, S. *J. Phys. Chem. Solids* **1974**, *35*, 555.

DOI: 10.1021/acs.inorgchem.5b00716
Inorg. Chem. 2015, 54, 7767−7773